Supplementary Material - Molecular Dynamics Simulations of Ultrafast Radiation Induced Melting at Metal-Semiconductor Interfaces

Ashwin Ravichandran,[1] Mohit Mehta,[1] Andrew A Woodworth,[2] and John W Lawson[3, a)]

[1)]*KBR Inc., Intelligent Systems Division, NASA Ames Research Center, Moffett Field, CA, 94035.*

[2)]*Materials and Structures Division, NASA Glenn Research Center, Cleveland, OH, 44135.*

[3)]*Intelligent Systems Division, NASA Ames Research Center, Moffett Field, CA, 94035.*

[a)]Author to whom correspondence should be addressed:john.w.lawson@nasa.gov

I. SUPPLEMENTARY MATERIAL

A. Discussion on the three scenarios corresponding to different incident energies

The initial electron temperatures corresponding to the three scenarios were calculated roughly considering the incidence of Xe particle with 30, 50, and 70 MeV energy, respectively, on tungsten (W) atoms. The stopping power for W were obtained from the SRIM tables[1] and the initial electron temperatures were calculated accordingly. Note that the above choices of energies are arbitrary and were only chosen to induce a large thermal shock on the lattice atoms and to ensure that the lattice temperatures of both SiC and W does not raise far beyond the corresponding melting temperatures, where the validity of the force field parameters might be questionable.

B. Comparing the local molecular structures of SiC classified by PointNet and VoroTop analysis

Fig. S1 and S2 shows the classification of a pure SiC slab using PointNet and VoroTop analysis, respectively, as regions of ordered and disordered structures. The representative snapshots are shown at 2 ps after the radiation strike. PointNet, as discussed in the main text, classifies the bulk of the SiC slabs as solid-like ordered (shown in light red) and also predicts disordered regions along the radiation track (shown in blue). On the other hand, the VoroTop analysis based classification (Fig. S2) fails to distinguish between the ordered and disordered regions and predicts the entire SiC slab as an unknown structure not belonging to FCC, BCC, or HCP lattices (shown in olive green).

C. Temperature evolution of electronic grids for Scenario I

The evolution of the average temperature of the electronic grids at the interface region is shown in Fig.S3 along with the corresponding lattice temperature. As expected, the energy from the radiation track rapidly dissipates away and the interface eventually cools down.

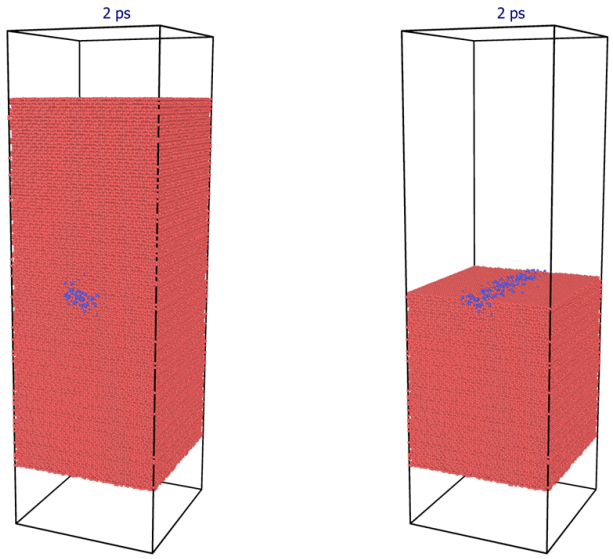

FIG. S1: Classification of SiC slab by PointNet, 2 ps after radiation impact. Left: Snapshot of the entire slab and right: Cross-section of the same along the radiation track. The ordered regions are shown in light red and the disordered regions are shown in blue.

D. Representative snapshots for Scenario I

Simulation snapshots of the W-SiC slab at different times and at conditions corresponding to Scenario I is shown in Fig. S4

E. Temperature evolution of electronic grids for Scenario II

The evolution of the average temperature of the electronic grids at the interface region for Scenario II is shown in Fig.S5 along with the corresponding lattice temperature.

F. Representative final snapshots of five different simulation runs under Scenario II conditions

The representative final snapshots after 3000 ps under the conditions corresponding to Scenario II is shown in Fig. S6.

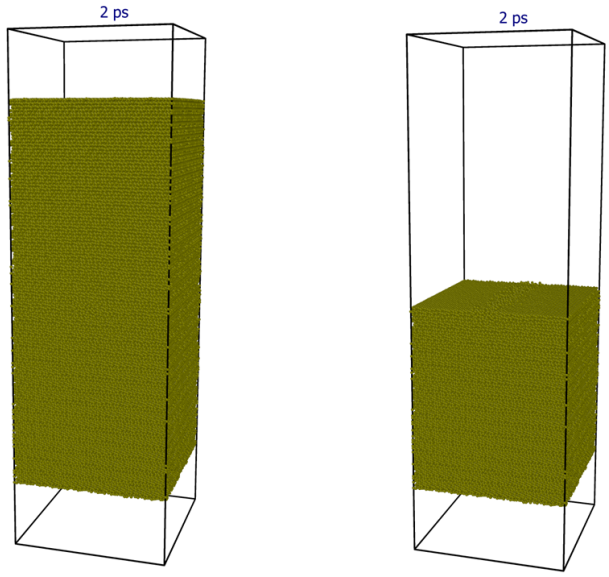

FIG. S2: Classification of SiC slab by VoroTop analysis, 2 ps after radiation impact. Left: Snapshot of the entire slab and right: Cross-section of the same along the radiation track. The regions classified by VoroTop analysis as unknown structures are shown in olive green.

G. Size of the largest W cluster at the interface for Scenario II

Size of the largest cluster at the interface region as a function of time is shown in Fig. S7. A cut-off of 3.5 Å (close to the lattice spacing of solid W) was used to determine the cluster size. The size of the largest solid cluster rapidly decreases and remains constant until the onset of nucleation at $\sim$ 140-150 ps.

H. SiC damage along the radiation track

Representative snapshot showing the cross-section view of the disordered SiC along the radiation track is shown in Fig. S8. The snapshot corresponds to Scenario II described in the main text.

I. Mean-squared displacement at high temperature

Mean-squared displacement (MSD) of W, Si, and C along the z direction at 2000 K are shown in Fig. S9. Note that the mean-squared displacement of the atoms were calculated at constant temperature and not during radiation strike. There is no noticeable diffusion of atoms normal to

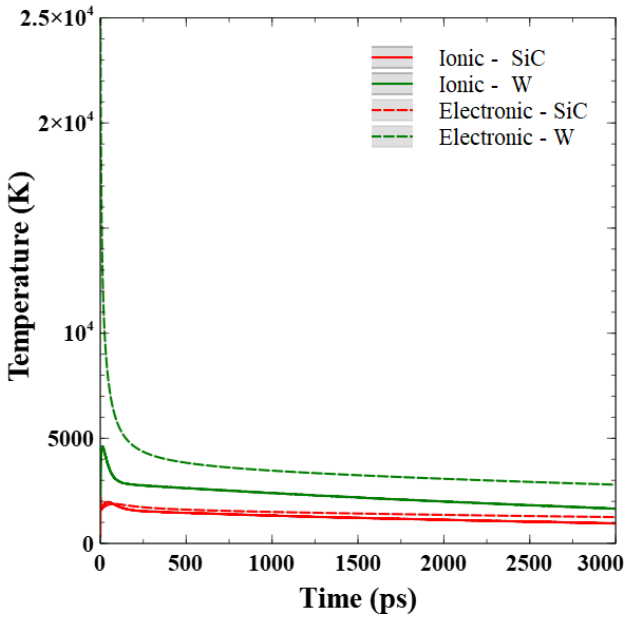

FIG. S3: Evolution of the temperature of the electronic grids at the interface for the simulation system corresponding to Scenario-I (dashed lines). The solid lines are the corresponding lattice temperature shown in the main text.

the interface at the time scale studied here.

J. Temperature evolution of electronic grids for Scenario III

The evolution of the average temperature of the electronic grids at the interface region for Scenario III is shown in Fig.S10 along with the corresponding lattice temperature. As expected, both the ionic and the electronic temperature are the highest (at any given instance) for this case when compared to the low energy and intermediate energy scenarios.

K. Onset of nucleation for Scenario III

The growth of the largest W cluster at the interface region with time is shown in Fig. S11 for Scenario III. Around $\sim$ 1000 ps there is a drastic increase in the cluster size, indicating the onset of recrystallization. The temperature of W at the interface around this time is $\sim$ 3950-3880 K that results in an observed undercooling of $\sim$ 700-770 K for the model.

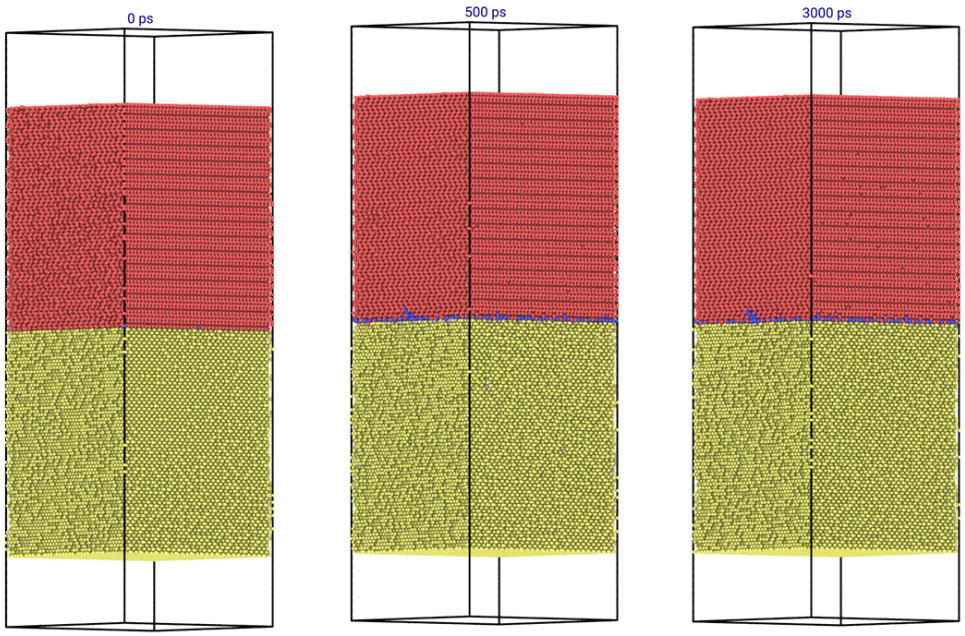

FIG. S4: Simulation snapshots of W-SiC slabs corresponding to Scenario I explained in the main text at 0, 500, and 3000 ps.

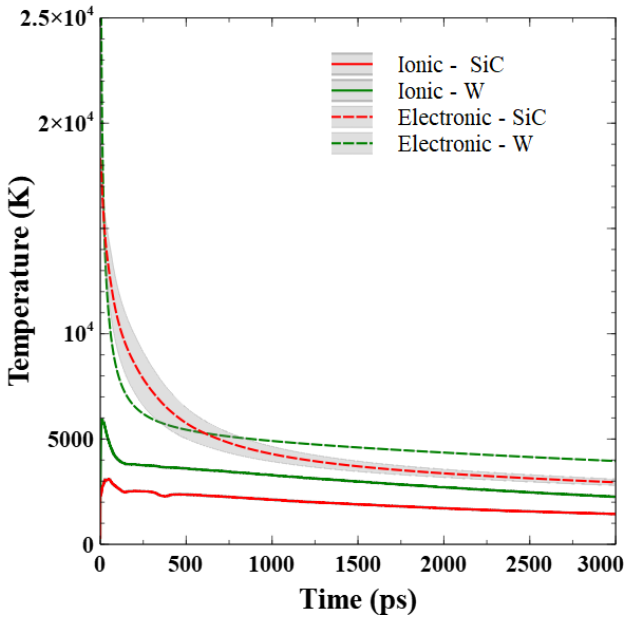

FIG. S5: Evolution of the temperature of the electronic grids at the interface for the simulation system corresponding to Scenario-II (dashed lines). The solid lines are the corresponding lattice temperature shown in the main text.

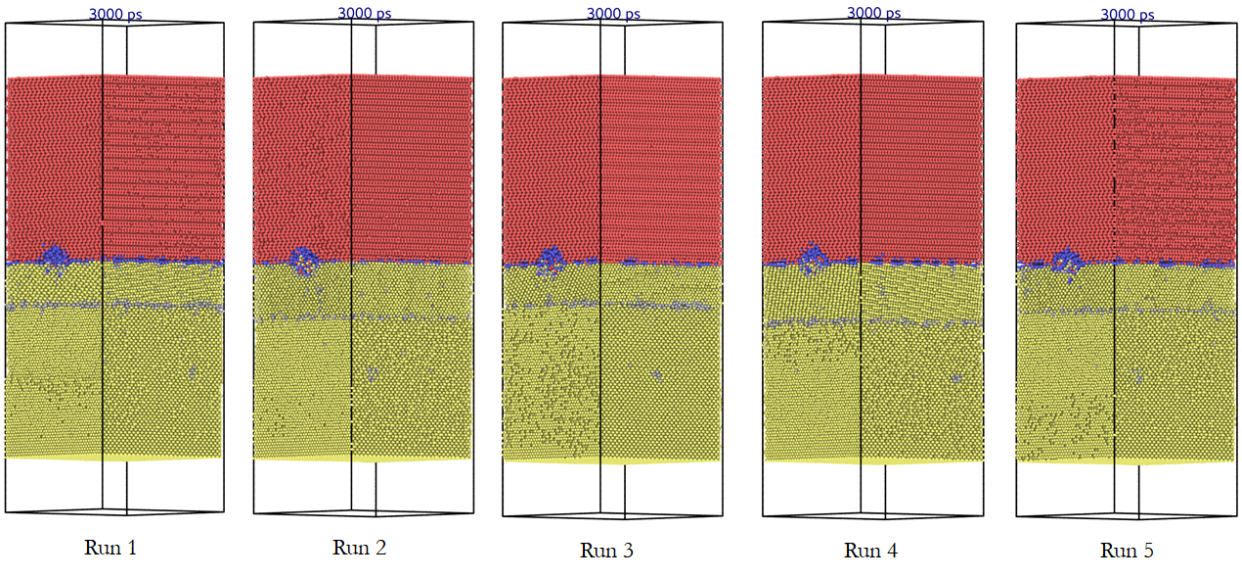

FIG. S6: Simulation snapshots of five different trajectories (Scenario II) showing the formation of a narrow band of disordered layer in W slabs (shown in gray) at the end of each simulation (3000 ps).

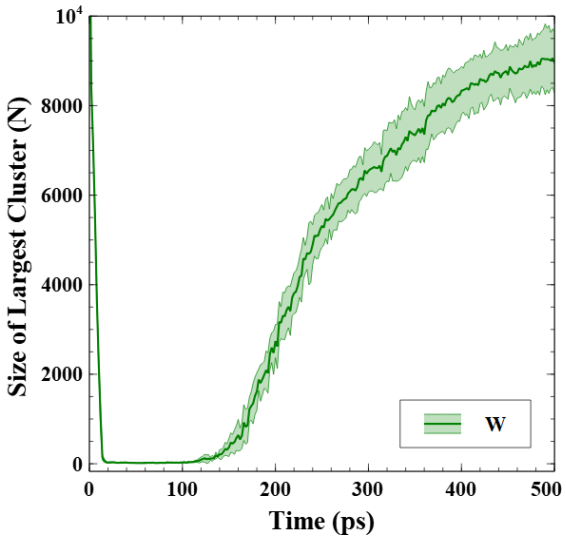

FIG. S7: Growth of the largest solid W cluster at the interface region for Scenario II described in the main text. The standard deviations in cluster size are shown as shaded regions.

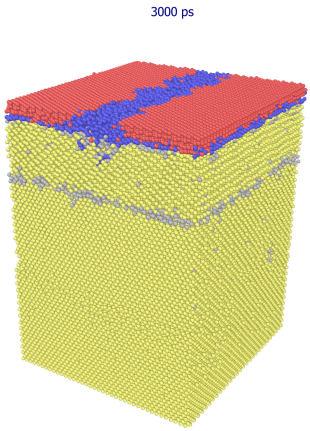

FIG. S8: Cross section view of SiC damage along the radiation track under the conditions corresponding to Scenario II at the end of the simulation run (3000 ps). Light red and blue atoms represent ordered and disordered SiC, respectively, while yellow and gray atoms represent ordered and disordered W, respectively. The simulation box boundary is not shown for clarity.

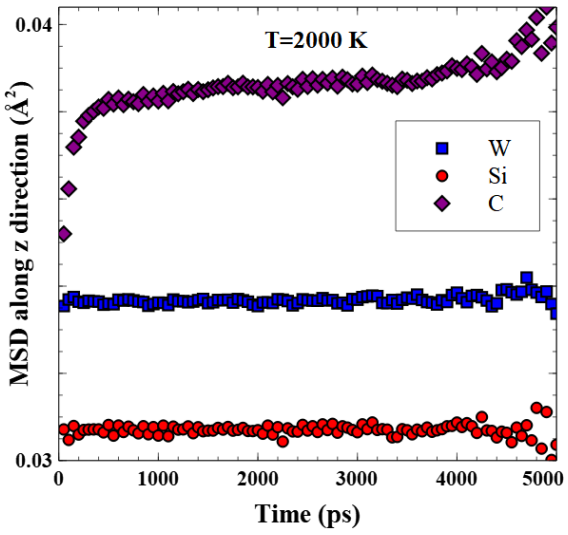

FIG. S9: Mean-squared displacement (MSD) of W, Si, and C atoms in the direction normal to the interface at a constant temperature of 2000 K.

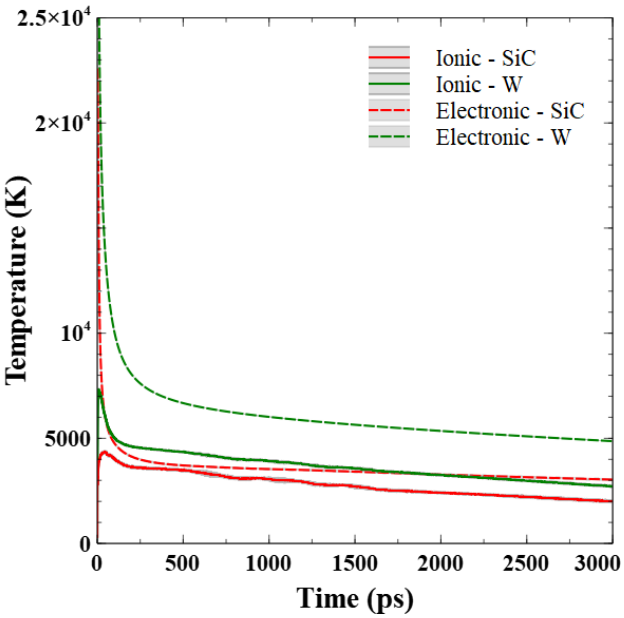

FIG. S10: Evolution of the temperature of the electronic grids at the interface for the simulation system corresponding to Scenario-III (dashed lines). The solid lines are the corresponding lattice temperature shown in the main text.

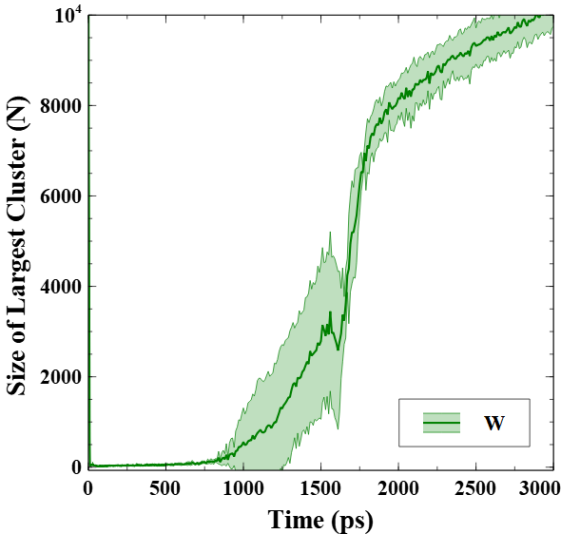

FIG. S11: Growth of the largest solid cluster of W at the interface region for Scenario III. The standard deviations in cluster size are shown as shaded regions.

REFERENCES

[1]J. Ziegler, M. Ziegler, and J. Biersack, "SRIM (http://www. srim. org/)," .